[3]Dokuchaev, L.V., "Plotting the Regions of Stable Rotaiton of a Space Vehicle with Elastic Rods," *Kosmicheskic Issledovdniya* (English Translation), Vol. 7, July-Aug. 1969, pp. 534-546.

[4]Brown, D.P. and Schlack, A.L., "Stability of a Spinning Body Containing an Elastic Membrane via Liapunov's Direct Method," *AIAA Journal*, Vol. 10, Oct. 1972, pp. 1286-1290.

[5]Levinson, D. and Kane, T.R., "Spin Stability of a Satellite Equipped with Four Booms," *Journa. of Spacecraft and Rockets*, to be published.

[6]Meirovitch, L., "Liapunov Stability Analysis of Hybrid Dynamical Systems with Multi-Elastic Domains," *International Journal of Non-Linear Mechanics*, Vol. 7, 1972, pp. 425-443.

[7]Meirovitch, L. and Calico, R., "The Stability of Motion of Force-Free Spinning Satellites with Flexible Appendages," *Journal of Spacecraft and Rockets*, Vol. 9, April 1972, pp. 237-245.

[8]Crespo Da Silva, M.R.M., "Attitude Stability of a Gravity-Stabilized Gyrostat Satellite," *Celestial Mechanics*, Vol. 2, 1970, pp. 147-165.

[9]Merovitch, L. and Calico, R.A., "A Comparative Study of Stability Methods for Flexible Satellites," *AIAA Journal*, Vol. 11, Jan. 1973, pp. 91-98.

Effect of Mass Addition on the Boundary Layer of a Hemisphere at Mach 6

A. Demetriades,* A. J. Laderman,† L. Von Seggern,‡
Aeronutronic Ford Corporation, Newport Beach, Calif.

A. T. Hopkins,§
SAMSO/RSSE, Los Angeles, Calif.

and

J. C. Donaldson¶
ARO, Inc., Tullahoma, Tenn.

Nomenclature

A	= surface area
D	= diameter of hemispherical tip
f_w	= nondimensional injection mass-flux
M	= constant in the mass-flux distribution [Eq. (1)]
$\dot{M}$	= total mass injected through hemisphere (mass per unit time)
$\dot{m}$	= local mass flux (mass per unit area and time)
N	= constant in the mass-flux distribution [Eq. (1)]
p_c	= hemisphere internal pressure
Re_{D_∞}	$= \rho_\infty u_\infty D/\mu_\infty$
Re_θ	= local momentum Reynolds number
S	= constant determined from the data [Eq. (2)]
u	= velocity parallel to model axis (or surface)
v	= velocity normal to model surface
β	= local pressure gradient
δ	= boundary-layer thickness
μ	= viscosity
ρ	= density
φ	= angle measured from stagnation point
$(\ )_e$	= at boundary-layer edge
$(\ )_T$	= at boundary-layer transition
$(\ )_w$	= wall properties
$(\ )_\infty$	= freestream properties

Received Jan. 20, 1976; revision received March 31, 1976. Work supported by USAF/SAMSO under Contract F04701-71-C-0035.

Index categories: Boundary Layers and Convective Heat Transfer—Laminar; Boundary-Layer Stability and Transition.

*Supervisor, Fluid Mechanics Section. Associate Fellow AIAA.
†Principal Scientist. Member AIAA.
‡Engineer.
§Project Engineer, Lieutenant, USAF.
¶Project Engineer.

Considerable theoretical work has been performed to examine boundary-layer development on blunt bodies at hypersonic speeds and the associated heat transfer with both passive-ablator and active-transpiration cooled materials. Direct experimental data, on the other hand, are scarce on the blunt body laminar boundary layer and on the conditions which cause transition to turbulence. This scarcity is, of course, due mainly to the obvious difficulties of probing the boundary layer near stagnation points. This Note presents boundary-layer development and transition results for a smooth spherically blunted cone with essentially zero heat transfer but with finite mass transfer rates.

The experiment was conducted in the 50-in. diameter Hypersonic Wind Tunnel B of the Arnold Engineering and Development Center (AEDC). A spherically blunted 5-deg half-angle cone with a 7-in. nose radius was operated adiabatically at a nominal Mach 6 continuous flow condition. The stagnation temperature was 390° F and supply pressures ranged from 160 to 280 psia ($3.86\times10^6 < Re_{D\infty} < 6.18\times10^6$). The spherical nose was built of porous sintered stainless steel with an effective permeability of $0.94\times10^{-9}\text{cm}^{-2}$, and was designed with a variable wall thickness to allow gas injection when its interior was pressurized. (Pressures, p_c, ranging up to 35 psia were used.) The resultant surface mass flux distribution was

$$\dot{m}(\varphi) = M\cos 2\varphi + N \tag{1}$$

so as to simulate the mass flux distribution on an ablating reentry body. In the present case the injectant was air at near-stagnation temperature. Typical values of M and N, for example at $p_c = 19.7$ psia, were 0.00675 and 0.00875 lb/ft² sec respectively.

For $\varphi > 40°$, the flow was surveyed by external probes lowered to the surface through the tunnel ceiling. At $\varphi = 10°$, 20° and 30°, probes were extended and retracted at will from the inside of the model, through 0.035″ diam holes on its surface. The internally actuated probes were either 0.002″ diam (etched down from 0.004″ diam tubing) and 0.010″ diam pitot probes or 0.00002″ diam hot wire anemometers. A complement of surface pressure taps, thermocouples, heat transfer gages, acoustic sensors and accelerometers was installed to provide additional flow data and to monitor the model behavior.

The boundary-layer profiles shown in Fig. 1 were derived from the pitot measurements assuming a constant-pressure layer with a linear total temperature change from the layer edge to the surface. Corresponding theoretical laminar flow profiles (Fig. 1) have been supplied by Bywater.[1] The agreement is judged adequate, especially if one considers the marginal resolution of the pitot probe at $\varphi < 30°$, where the boundary-layer thickness was no more than 10 times larger than the probe diameter. Similarly, the measured boundary-

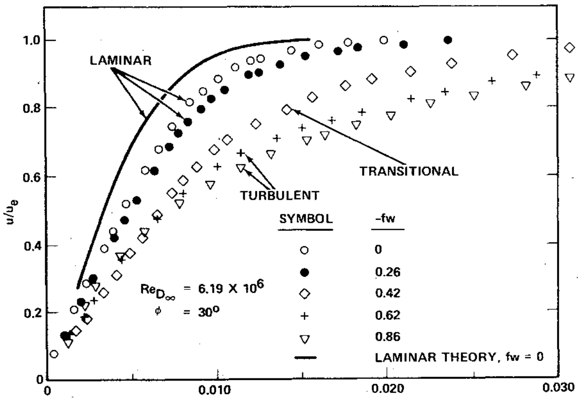

Fig. 1 Boundary-layer velocity profiles for various mass injection rates.

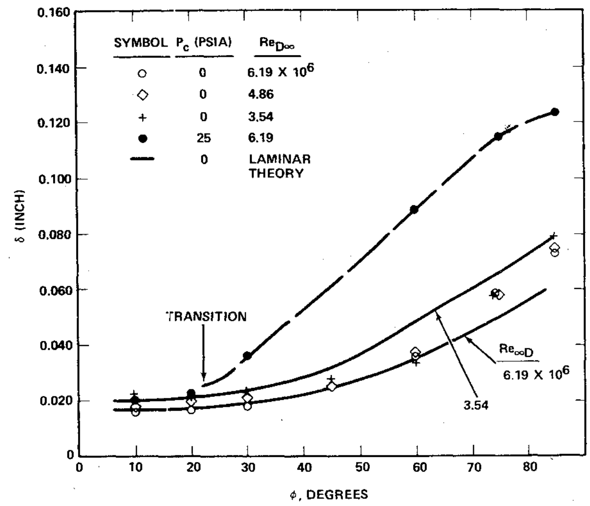

Fig. 2 Boundary-layer growth with and without injection.

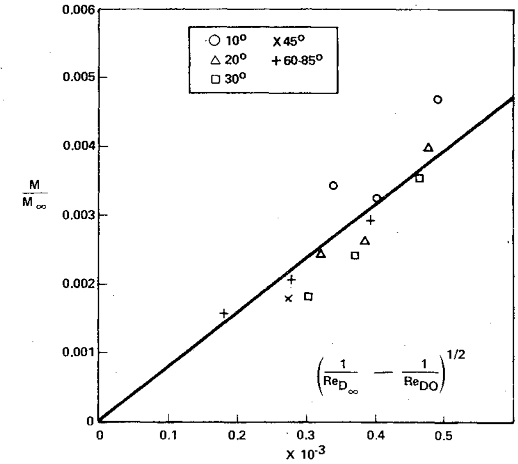

Fig. 3 Relation between the integrated mass flow, the resulting location of transition (in degrees from the stagnation point) and the hemisphere Reynolds number $Re_{\infty D}$.

layer thickness δ was close to the theoretical prediction, as shown on Fig. 2. Although a precise assessment of the measurement error in these profiles was not made, it was concluded that the theoretical predictions of laminar boundary-layer growth are satisfactory as represented in modern computer codes.[1]

When the mass addition rate exceeded a certain threshold at each flow Reynolds number, the boundary-layer became turbulent. This was evidenced not only by the profile changes and boundary-layer thickening (see Figs. 1 and 2) but most strikingly by the turbulence detected by the hot wire anemometers. From such data the transition location could be correlated by

$$\varphi_T = 893\left[\frac{1}{Re_{D_\infty}} - \left(\frac{1}{S}\frac{\dot M}{\dot M_\infty}\right)^2\right]10^6 - 30(\text{degrees}) \quad (2)$$

with

$$\dot M_\infty = \frac{\pi D^2}{4}\rho_\infty u_\infty \text{ (subtended mass flow)}$$

$$\dot M = \int_A \dot m \, dA \text{ (total mass flow rate ejected)} \quad (3)$$

Implicit in this criterion is a data "correlation" for smooth, adiabatic hemispheres without mass addition which relates the angular transition location to the hemisphere Reynolds number as follows

$$\frac{1}{Re_{D_\infty}\,(\dot M=0)} = (0.036+0.00112\varphi)+10^{-6}\ (\varphi \text{ in degrees}) \quad (4)$$

It should be stressed that this correlation is used here only as an approximation for the nonblowing limit and does not address subtle questions such as the effect of unit Reynolds number and freestream turbulence.

A linear least squares computer fit of all the data in Fig. 3 showed that the constant $S = 8.0$, as represented by the slope of the straight line on that figure. Slightly better agreement can be achieved if individual curve fits for each angle φ are performed, in which cases S varies from about 7 to about 9.

Theoretical considerations lead to the belief that mass addition increases the laminar boundary-layer thickness and simultaneously introduces changes in the velocity profile. By computing the increase in the momentum thickness Reynolds number Re_θ caused by the small but discernible thickening of the pretransitional layer (Fig. 2) it was tentatively concluded that the observed acceleration of transition with blowing could be explained in terms of this thickening alone. It is a much more difficult task to discern small velocity profile changes from the recorded data; this would of course, be a crucial step in predicting the observed transition results from the viewpoint of hydrodynamic stability.

A second important conclusion drawn from Figs. 1 and 2 is that the mass addition rates needed to cause transition are small. The mass addition parameter

$$|f_w(\varphi)| \equiv \frac{(\rho v)_w}{(2\rho_e\beta_e\mu_e)^{1/2}} \quad (5)$$

was found to be at most of order 1. Theoretical efforts to predict "massive blowing" effects are based on laminar flow theory with f_w of order 10 or higher.[2] Therefore, it appears that, since the laminar boundary layer cannot support these large injection rates, the laminar flow computations dealing with such large rates should be reformulated to include the effect of turbulent mixing in the boundary layer.

References

[1] Bywater, R., Aerospace Corp., Los Angeles, Calif., private communications 1974-1975.

[2] Libby, P. A., "The Homogeneous Boundary Layer At An Axisymmetric Stagnation Point With Large Rates of Injection," *Journal of the Aeronautical Sciences*, Vol. 29, Jan. 1962, p. 48.

Statistical Analysis of Trim Maneuvers in Low-Thrust Interplanetary Navigation

George C. Rinker,* Robert A. Jacobson,†
Jet Propulsion Laboratory, Pasadena, Calif.
and
Lincoln J. Wood‡
Hughes Aircraft Company, El Segundo, Calif.

I. Introduction

ONE of the proposed applications of solar electric propulsion is the exploration of comets and asteroids. In order to effectively employ solar electric propulsion in flights to these bodies, difficult navigation problems must be over-

Presented as Paper 75-85 at the AIAA 13th Aerospace Sciences Meeting, Pasadena, Calif., January 20-22, 1975; submitted February 24, 1975; revision received December 22, 1975. This paper presents the results of one phase of research carried out at the Jet Propulsion Laboratory, California Institute of Technology, under contract NAS7-100, sponsored by NASA.

Index categories: Navigation, Control, and Guidance Theory; Spacecraft Navigation, Guidance, and Flight-Path Control Systems.

*Engineer, Mission Analysis Division. Associate Member AIAA.

†Senior Engineer, Mission Analysis Division. Member AIAA.

‡Staff Engineer. Formerly Bechtel Instructor in Engineering, California Institute of Technology, and Consultant, Jet Propulsion Laboratory. Member AIAA.